

POWDER COMPACTION IN THE AXISYMMETRIC CASE

Andrey E. Buzjurkin

Sergey P. Kiselev

buzjura@itam.nsc.ru

Abstract. The interaction between shock waves in porous and powdered materials remains an important research area. This importance stems from the necessity of establishing optimum loading conditions for obtaining compacts with spatially uniform physical and mechanical properties.

The present consideration shows that an increase in the decay time of the external pressure achieved either through increasing the explosive thickness or through increasing the value of the external load causes no decrease in the dimensions of the fractured region under a fixed value of detonation velocity. At the same time, as the propagation velocity of the detonation wave decreases, the fractured region shrinks substantially.

1 Introduction

Investigation into the interaction between oblique shock waves in porous materials and powders is a topical problem in optimization of loading conditions for obtaining, from a given sample, a compacted material with spatially uniform physical and mechanical properties. In compacting a powder in the cylindrical scheme, an irregular interaction between shock waves occurs. The compacted powder displays substantial non-uniformity in particle displacements, resulting in inhomogeneity of powder characteristics and, in some cases, even in material failure.

In compacting porous material and powders, the strong bonding between particles is achieved through the combined pressure-shear loading. During the compacting, a substantial energy is released at the interfaces between powder particles, resulting in surface cleaning and material melting in narrow interfacial regions. As a result, pore collapsing, giving rise to strong bonding between particles, occurs. Below, this phenomenon is termed compaction.

V.F. Nesterenko proposed the following criterion for the formation of a strong compact:

$$P > 2H_V, \quad (1)$$

where, according to [1], $H_V \approx 3Y_s$. Following [1], we can write criterion (1), deduced from experimental data, as

$$P > 6Y_s. \quad (2)$$

In turn, R. Prummer [2] uses the following condition for obtaining a uniform, in its physical properties, cylindrical compact with no Mach reflection induced singularities at its center: $P \approx H_V$, where P is the detonation pressure. Comparing condition (1) with the condition $P \approx H_V$, Nesterenko [1] arrives at a conclusion that it is impossible in principle, without a central rod, to obtain a spatially uniform compact in the cylindrical loading scheme since the shock pressure required for obtaining a dense compact (2) will always lead to Mach reflection at the center of the sample.

Another important problem is preservation of the finish compact after loading. With the arrival of unloading waves, there arises a tensile stress that results in partial or complete destruction of the sample. We assume that the sample undergoes mechanical failure if the maximum tensile stress σ_{max} reaches a certain critical value σ_* . In line with the adopted hypothesis, the following condition for the sample failure should be assumed:

$$\sigma_{max} > \sigma_*, \quad (3)$$

where σ_{max} is the highest stress among the principal stresses for the strained state under study and σ_* is the critical stress.

In the present work, the critical stress σ_* is estimated as $\sigma_* = (2/3)Y_s \ln(1/m_1)$, where m_1 is the residual porosity. Taking the finish-compact density to equal 99%, we obtain $m_1 = 0.01$ and $\sigma_* \approx 3Y_s$. For the principal stresses, we have:

$$\sigma_1 = \frac{\sigma_{xx} + \sigma_{yy}}{2} \pm \frac{1}{2} \sqrt{(\sigma_{xx} - \sigma_{yy})^2 + 4\sigma_{xy}^2}, \quad \sigma_3 = \sigma_{\theta\theta}.$$

2 Calculation results and discussion

In order to gain a better insight into the effect of loading conditions and, in particular, to study the effect of detonation velocity, explosive thickness, and explosion pressure on the properties of the final sample, we numerically solved the problem about powder compaction in the axisymmetric case. The problem statement is clear from Fig. 1. We solved the full system of equations governing the deformation of a porous elastic-plastic material. The action of the explosion products on the sample was modeled with a pressure applied to the upper border of the sample. The pressure was calculated by the approximation formula for the pressure upon unrestricted dispersion of detonation products [4]:

$$P(t) = P_H \exp(-(t - x/D)/t_1), \quad t_1 = \sqrt{\frac{3(\gamma_e + 1) \delta_e}{4(\gamma_e - 1) D}}.$$

Here δ_e is the explosive thickness and γ_e is the adiabatic exponent of the detonation products. At the lower border of the sample, the rigid-wall condition was set, and the right border was stress-free. At the left border, the rigid-wall condition was assumed.

In the calculations, the scheme proposed by Wilkins [3] for aluminum powders of various initial porosities was used. The shock wave propagated from left to right. In the calculations, the values of parameters were as follows: $\rho_s = 2.71 \text{ g/cm}^3$, $Y_s = 0.0041 \text{ Mbar}$, $K_s = 0.744 \text{ Mbar}$, and $\mu_s = 0.248 \text{ Mbar}$.

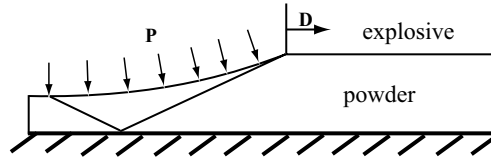


Figure 1: Problem statement

Figure 2, a and b shows the pressure isolines for the cases of planar and cylindrical symmetries with identical loading conditions. It is seen from Fig. 2 that, in the planar statement of the problem, a regular reflection of the incident shock wave takes place. In the case of the cylindrical loading scheme, the incident shock waves bends as it approaches the cylinder axis, and, under the same loading conditions, an irregular reflection occurs.

Figure 3, a shows the pressure profile near the symmetry axis for the cases of planar and cylindrical statements (solid and dashed curves, respectively). An appreciable pressure rise near the symmetry axis is observed in the case of cylindrical configuration compared to the planar problem due to the divergence of the shock wave to the axis.

Figure 3, b shows the profile of the longitudinal velocity u_x across the sample under loading behind the shock front. The solid and dashed lines show the data for the planar and axisymmetric problem statements, respectively. It is clearly seen that the velocity in the cylindrical case is much greater than in the planar variant.

As stated above, an important problem is preservation of finish compact, i.e., preventing its mechanical failure and obtaining a sample with uniform properties. Using criterion (3), we can find the interface between the solid and destructed materials. It should be emphasized that in derivation of (3), it was implicitly assumed that the interfacial melted zones are narrow, and the material in these zone rapidly solidifies as the particles in the bulk of the material undergo cooling. If this condition does not hold, then there can be a situation in which, by the moment of arrival of the unloading wave, the material in the interfacial zones still remains melted, which will prevent compaction. In this case, the dimensions of the destruction region will be dependent on the loading decay time and on the explosive thickness.

The explosive thickness should be large enough to prevent shock wave damping in the powder and to enable complete pore collapsing in the sample. The density isolines for the explosive thickness $\delta_e = 1 \text{ cm}$

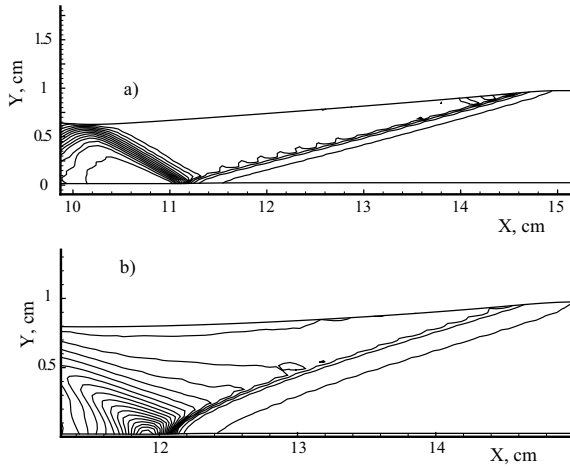


Figure 2: Pressure isolines: a) — planar geometry; b) — cylindrical configuration

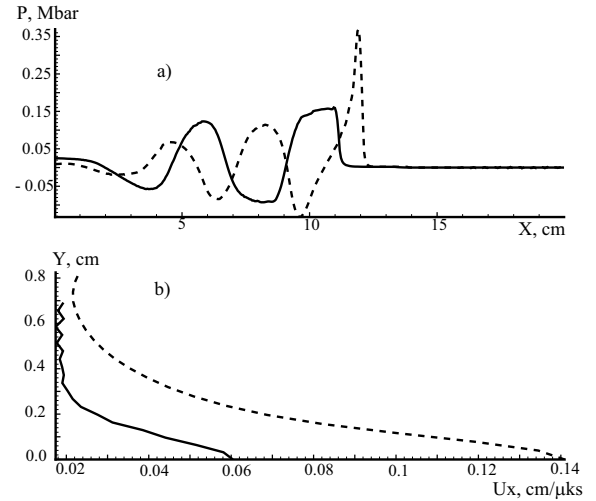


Figure 3: Pressure profile (a) and longitudinal-velocity profile $u_x(y)$ (b).

and the external pressure $P = 0.05$ Mbar are shown in Fig. 4, a and b. Parts a and b of this figure shows the calculation data for the axisymmetric and planar statements, respectively. It is clearly seen that in the case of cylindrical symmetry the shock wave bends near the axis, giving rise to an irregular reflection; in the planar configuration, a regular interaction occurs. Figure 5, which depicts the distribution of porosity m_1 across the sample compacted in the cylindrical geometry (the dashed line in Fig. 5), is indicative of complete collapsing of pores over the entire thickness of the sample. In the planar case (see the dashed line in Fig. 5), the complete collapsing of pores is observed approximately over half the thickness of the sample, and the porosity near the symmetry axis is close to the initial one, m_1^0 .

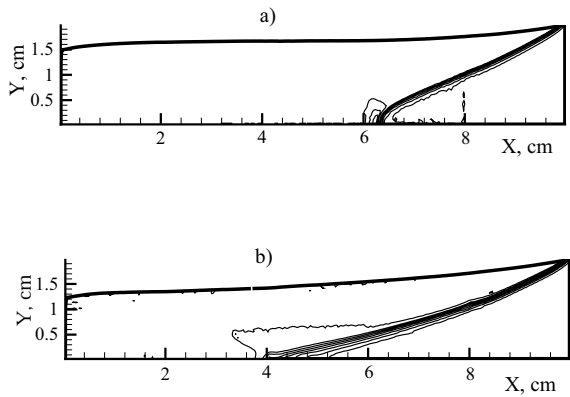


Figure 4: Density isolines for $\delta_e = 1$ cm: a) — cylindrical configuration; b) — planar configuration

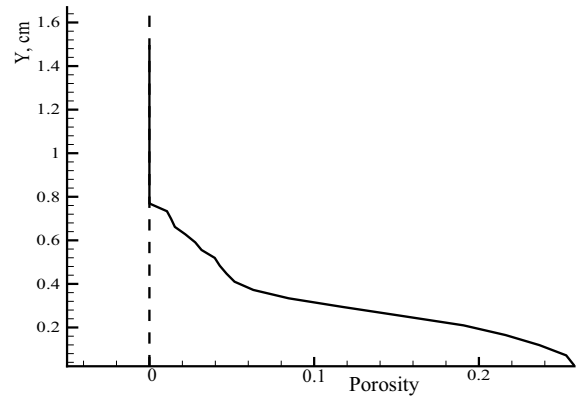


Figure 5: Porosity m_1 for $\delta_e = 1$ cm: solid line — planar statement; dashed line — cylindrical configuration

The density isolines for the explosive thickness $\delta_e = 2$ cm are shown in Fig. 6, a and b. The external pressure was taken to be $P = 0.05$ Mbar. Parts a and b of this figure show the calculation data for the axisymmetric and planar statements. In the cylindrical case (see Fig. 6, a), an irregular reflection is clearly observed, whereas in the planar case (see Fig. 6, b) the incident shock wave interacts with the rigid wall in the regular manner. In both cases, all pores in the sample collapse completely.

Further calculations were carried out for the explosive thicknesses $\delta_e = 2$ cm, $\delta_e = 3$ cm, and $\delta_e = 5$ cm.

Figure 7, a and b illustrates the effect of applied pressure on the dimensions of the destruction region. In the calculations, the external pressures were $P = 0.05$ Mbar and $P = 0.075$ Mbar, respectively, and the detonation velocity in both cases was $D = 0.7$ cm/msec. The solid and dashed lines show the

data for the explosive thicknesses $\delta_e = 3$ cm and $\delta_e = 5$. Regions 1 and 2 are the compacted and destruction regions. As is seen from the figure, an increase in the external load causes no shrinkage of the destruction zone. Thus, it can be concluded that an increase in the decay time of the pressure applied to the sample resulting from an increase in the explosive thickness or in the value of the external load does not make the destruction zone shrink at a fixed propagation velocity of the detonation wave.

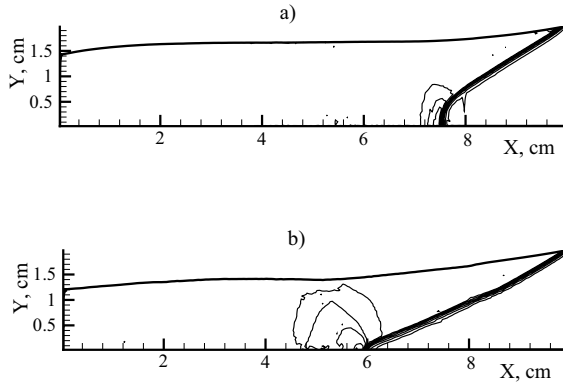


Figure 6: Density isolines for $\delta_e = 2$ cm: a) — cylindrical configuration; b) — planar statement

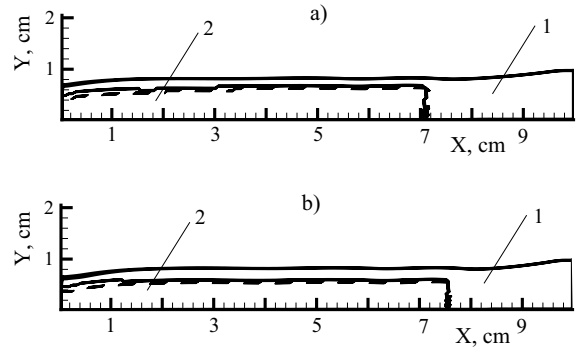


Figure 7: Compacted and destroyed regions for two values of external pressure, $P = 0.05$ Mbar (a) and $P = 0.075$ Mbar (b).

A decrease in the velocity of the detonation wave results in a considerable shrinkage of the destruction region. Figure 8 show the compacted (1) and destroyed (2) regions in the sample for the detonation velocities $D = 0.3, 0.5, 0.7$ cm/msec at a fixed explosive thickness $\delta_e = 5$ cm and at a fixed external pressure $P = 0.05$ Mbar. The solid, dashed, and dot-and-dash lines show the calculation data for the detonation velocities $D = 0.3$ cm/msec, $D = 0.5$ cm/msec, and $D = 0.7$ cm/msec.

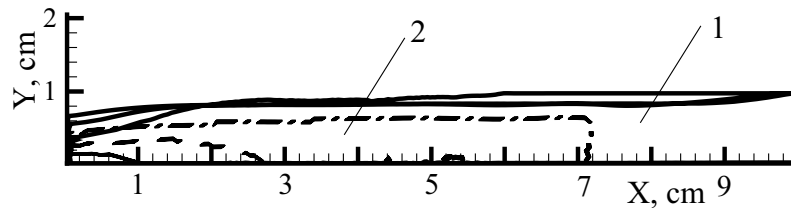


Figure 8: Compacted (1) and destroyed (2) regions.

The isolines of pressure for the indicated loading parameters are shown in Fig. 9, a–c. It is seen from the graphs that, as the shock-wave propagation velocity increases, the angle of incidence decreases and the reflected shock causes material destruction (see Fig. 9, b and c). As the velocity of the detonation wave increases, the angle of incidence of the incident shock wave increases and, as it is seen from Fig. 9, a, at the velocity $D = 0.3$ cm/msec the incident shock wave is close to the normal shock and the amplitude of the reflection wave is almost zero.

Since in the case of cylindrical symmetry no regular reflection occurs, the final sample turns out to be inhomogeneous. Figure 10 shows the distribution of the longitudinal velocity u_x (fig. 10, a) and temperature T (fig. 10, b) across the sample in the compacted region for the detonation velocity $D = 0.5$ cm/msec. An appreciable non-uniformity in the distribution of parameters is evident from the graphs. Near the axis, both the velocity and temperature are greater than in the region some distance away from it.

Parts a and b of Fig. 11 show the distributions of the longitudinal velocity u_x and temperature T across the compacted region of the sample predicted for the detonation velocity $D = 0.3$ cm/msec. Here, under identical loading parameters, the final sample is quite homogeneous.

As a result, it becomes possible to obtain spatially uniform compacted samples. The necessary condition for this is sufficiently low detonation velocity, equal, for the aluminum powder, to 0.3 cm/msec. Here, on the one hand, compaction condition (1) should be fulfilled and, on the other, the uniformity of loading parameters across the sample should be ensured.

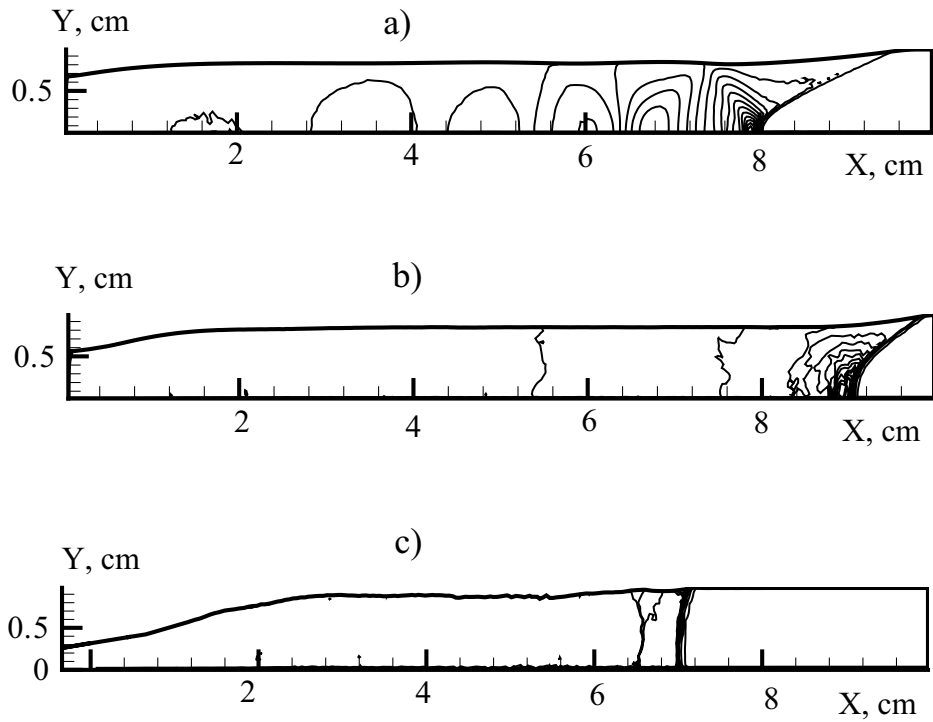


Figure 9: Pressure isolines: a) — detonation velocity $D = 0.7$ cm/msec; b) — detonation velocity $D = 0.5$ cm/msec; c) — detonation velocity $D = 0.3$ cm/msec

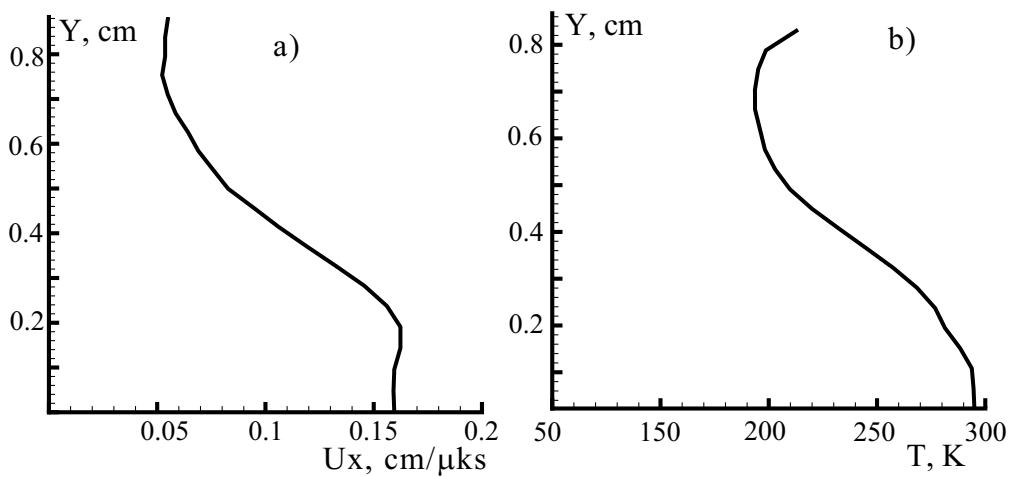


Figure 10: Predicted distributions of the longitudinal velocity u_x (a) and temperature T (b) across the compacted region of the sample for the detonation velocity $D = 0.5$ cm/msec

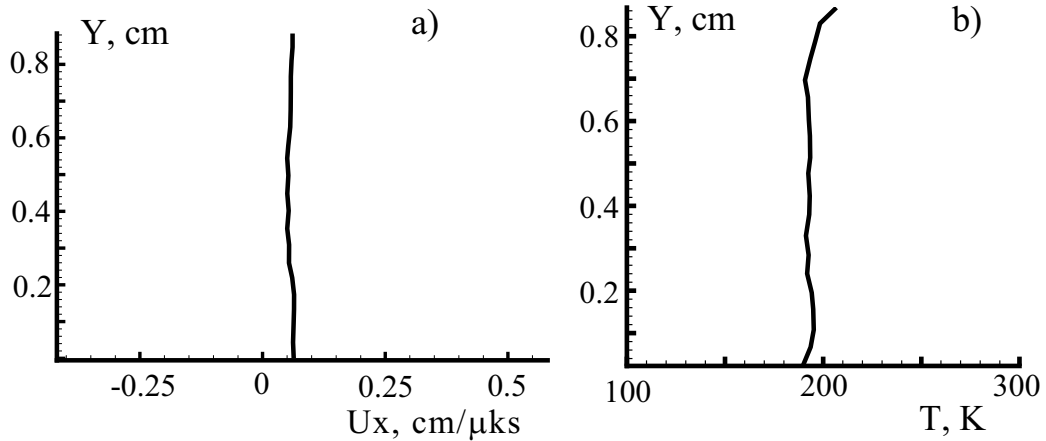


Figure 11: Distributions of the longitudinal velocity u_x (a) and temperature T (b) across the compacted region of the sample for the detonation velocity $D = 0.3$ cm/msec

Thus, the compaction of powders with low detonation velocities results in a considerable shrinkage of destruction zones in finish samples and in spatial uniformity of material parameters in their compacted parts.

The performed analysis shows that an increase in the decay time of the pressure applied to the sample due to an increase of the explosive thickness or the external loading causes no shrinkage of the destructed region at a fixed propagation velocity of the detonation wave. Simultaneously, a decrease in the propagation velocity of the detonation wave results in an appreciable shrinkage of this region.

3 Conclusions

The following conclusions can be drawn from the present study of powder compaction under shock pressing in the axisymmetric case. An increase in the pressure decay time due to increasing either the explosive thickness or the external loading intensity causes no shrinkage of the destruction zone at a fixed propagation velocity of the detonation wave. Compaction of powders with low detonation velocities results in a considerable shrinkage of destruction zones in finish samples and in a uniform distribution of material parameters in the compacted region.

Acknowledgements

The authors would like to express their gratitude to the Russian Science Support Foundation.

References

- [1] Nesterenko V.F. High-rate deformation of heterogeneous materials. - Novosibirsk: Nauka, 1992. – 284 p.
- [2] Prümmer R. Powder compaction // Explosive welding, forming and compaction / Ed. T.Z. Blazinsky. – London; New York: Appl. Sci. Publ., 1983. – P.381.
- [3] Wilkins M.L. Calculation of elastic-plastic flows // Fundamental Methods in Hydrodynamics. – Moscow: Mir, 1967. – P.212–264.
- [4] Pai V.V., Kuz'min G.E., Yakovlev I.V. Approximate estimation of loading parameters in composite materials loaded with intense shocks // Combustion, Explosion, and Shock Waves, 1995. Vol.31, No.3. P.124–130.

Andrey E. Buzjurkin, Novosibirsk, Russian Federation

Sergey P. Kiselev, Novosibirsk, Russian Federation